Membrane potential depolarization decreases the stiffness of vascular endothelial cells

Chiara Callies[1,*], Johannes Fels[1], Ivan Liashkovich[1], Katrin Kliche[2], Pia Jeggle[1], Kristina Kusche-Vihrog[1] and Hans Oberleithner[1]

[1]Institute of Physiology II, University of Münster, Robert-Koch-Str. 27b, 48149 Münster, Germany
[2]Department of Internal Medicine D, Albert-Schweitzer-Str. 33, 48149 Münster, Germany
*Author for correspondence (ccallies@web.de)

Accepted 2 February 2011
Journal of Cell Science 124, 1936-1942

doi:10.1242/jcs.084657

Summary

The stiffness of vascular endothelial cells is crucial to mechanically withstand blood flow and, at the same time, to control deformation-dependent nitric oxide release. However, the regulation of mechanical stiffness is not yet understood. There is evidence that a possible regulator is the electrical plasma membrane potential difference. Using a novel technique that combines fluorescence-based membrane potential recordings with atomic force microscopy (AFM)-based stiffness measurements, the present study shows that membrane depolarization is associated with a decrease in the stiffness of endothelial cells. Three different depolarization protocols were applied, all of which led to a similar and significant decrease in cell stiffness, independently of changes in cell volume. Moreover, experiments using the actin-destabilizing agent cytochalasin D indicated that depolarization acts by affecting the cortical actin cytoskeleton. A model is proposed whereby a change of the electrical field across the plasma membrane is directly sensed by the submembranous actin network, regulating the actin polymerization:depolymerization ratio and thus cell stiffness. This depolarization-induced decrease in the stiffness of endothelial cells could play a role in flow-mediated nitric-oxide-dependent vasodilation.

Key words: Actin cytoskeleton, Atomic force microscopy, Bis-oxonol, Cell stiffness, Electrical membrane potential, Endothelium

Introduction

Vascular endothelial cells line the interior surface of blood vessels and are, hence, directly subjected to the physical forces exerted by the flow of blood and blood pressure (Ali and Schumacker, 2002; Califano and Reinhart-King, 2010). To withstand these forces it is conceivable that they have to be both mechanically robust and, to a certain degree, compliant (Malek and Izumo, 1996; Michiels, 2003). The mechanical properties of endothelial cells also determine the endothelium-dependent control of vascular tone and, hence, blood pressure because they influence the endothelial production of the vasodilating gas nitric oxide (NO); stiff endothelial cells produce little NO, whereas less-stiff cells increase their NO production (Fels et al., 2010; Kidoaki and Matsuda, 2007; Oberleithner et al., 2007; Oberleithner et al., 2009).

Despite the importance of mechanical stiffness for endothelial performance, it is not yet fully understood how cell stiffness is regulated. In previous experiments, we have found that a variety of different treatments that should alter the endothelial plasma membrane potential (e.g. variation of the extracellular K^+ concentration) also alter the mechanical stiffness of the cells (Callies et al., 2009; Kusche-Vihrog et al., 2010; Oberleithner et al., 2006; Oberleithner, 2007; Oberleithner et al., 2007; Oberleithner et al., 2009). It is, hence, probable that, in all these cases, the possible change in membrane potential accounts for the observed stiffness changes and that the membrane potential in general regulates the mechanical properties of endothelial cells. It is possible that changes in the electrical field (E-field) across the plasma membrane affect the polymerization status of the submembranous actin network, which is well-known to be an important contributor to the mechanical stiffness of a cell (Hofmann et al., 1997; Kasas et al., 2005; Oberleithner et al., 2009; Rotsch and Radmacher, 2000; Wakatsuki et al., 2001). Several studies also support such a link between electrical potential changes and cellular actin organization (Chifflet et al., 2003; Luther and Peng, 1983; Meggs, 1990).

In order to test the hypothesis of a relationship between membrane potential and cell stiffness, we wanted to directly relate changes in the endothelial electrical plasma membrane potential difference to changes in cell mechanical stiffness. To this end, the membrane potential was manipulated in different ways and the induced potential changes were then simultaneously measured together with changes in cell stiffness. Simultaneous electrical potential and mechanical stiffness measurements in single cells were made possible by a novel technique that was recently developed in our laboratory (Callies et al., 2009). This technique involves a single setup of an atomic force microscope attached to an inverted fluorescence microscope and combines atomic force microscopy (AFM)-based stiffness measurements with fluorescence-based (bis-oxonol) membrane potential measurements.

Here, we show that three different depolarizing procedures, namely (i) increasing extracellular K^+ concentration ($[K^+]_e$) and, by this, decreasing the driving force for K^+ efflux; (ii) blocking K^+ channels using $BaCl_2$, so that the permeability of the membrane for K^+ is lowered; and (iii) decreasing extracellular Cl^- concentration ($[Cl^-]_e$) and, hence, increasing the driving force for Cl^- efflux, lead to a similar and significant decrease (~20%) in the mechanical stiffness of endothelial cells. Moreover, we demonstrate that it is the membrane potential depolarization and not cell swelling that causes the stiffness decrease of the cells under all three depolarizing conditions. We provide evidence that the cortical actin cytoskeleton is involved in the molecular mechanism by which the membrane potential affects cell stiffness.

Journal of Cell Science

Results

Membrane potential and stiffness changes upon high $[K^+]_e$

A relationship between the electrical membrane potential and the mechanical stiffness of endothelial cells was tested by altering the electrical potential in different ways while mechanical stiffness was simultaneously measured. The first experimental approach was a decrease in the electrochemical transmembrane driving force for K^+ by increasing the extracellular concentration of K^+ from 4 mM to 8 mM, which should depolarize cells. However, increasing $[K^+]_e$ can also result in membrane hyperpolarization; endothelial cells possess inwardly rectifying K^+ channels (K_{ir}) that act as 'K^+ sensors' and thus (paradoxically) cause hyperpolarization of the membrane potential in response to high $[K^+]_e$ (Nilius and Droogmans, 2001). We found that increasing $[K^+]_e$ from 4 to 8 mM leads to cell depolarization concomitant with a decrease in cell stiffness (cell softening) (Fig. 1). At 4 mM K^+, the membrane potential of the cells was –76.5±1.78 mV and depolarized by about 10 mV, to –66.5±1.29 mV, when extracellular K^+ was elevated to 8 mM. At the same time, cell stiffness decreased by ~20%, from 2.0±0.2 pN/nm at 4 mM to 1.6±0.15 pN/nm at 8 mM K^+. The results, hence, show that K^+-induced cell depolarization is accompanied by cell softening.

Effect of $BaCl_2$ and low $[Cl^-]_e$ on membrane potential and stiffness

In order to test further the relationship between membrane potential and stiffness, we manipulated the endothelial electrical potential by two alternative mechanisms, namely (i) by blocking K^+ channels with $BaCl_2$, so that the permeability of the membrane for K^+ is lowered (Fig. 2); and (ii) by decreasing $[Cl^-]_e$, thus increasing the driving force for Cl^- efflux (Fig. 3). Both methods should lead to a depolarization of the electrical membrane potential. We indeed observed a cell depolarization using $BaCl_2$ (from –72.6±1.86 mV to –52.9±2.08 mV) and, in parallel, a 25% decrease in endothelial mechanical cell stiffness, from 1.8±0.19 pN/nm to 1.3±0.13 pN/nm (Fig. 2). Upon decreasing $[Cl^-]_e$, endothelial cells also depolarized, from –70.8±4.27 mV to –45.4±7.02 mV. At the same time, the cells softened (from 1.6±0.18 pN/nm to 1.2±0.13 pN/nm) (Fig. 3).

Taken together, three distinct ways of depolarizing the plasma membrane potential all led to similar and significant decreases (P<0.05) in cell stiffness. The reversibility of these depolarizing procedures was also tested and we found that the induced membrane potential changes were indeed reversible. Likewise, the

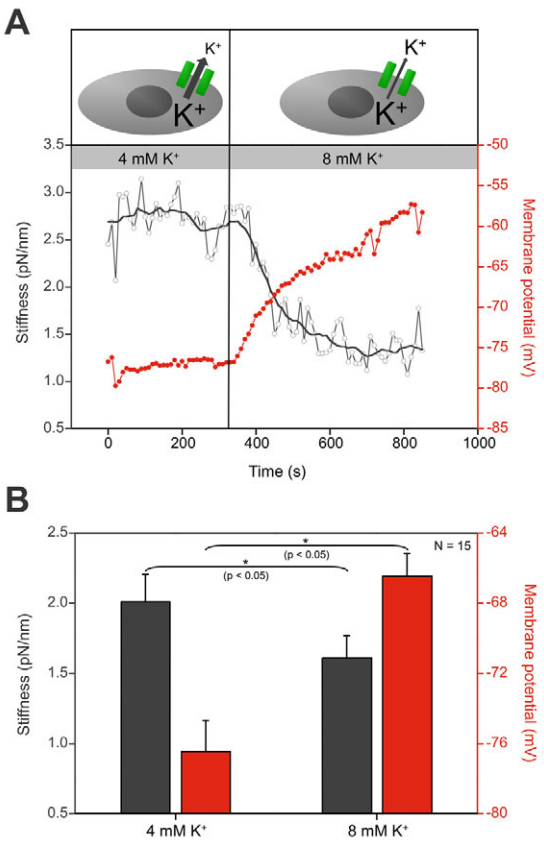

Fig. 1. Effect of high extracellular $[K^+]$ on membrane potential and stiffness. (**A**) Original tracing of one simultaneous membrane potential (red line) and stiffness (gray line) recording obtained in an individual cell subjected to a change in $[K^+]_e$ (from 4 mM to 8 mM). An increase in $[K^+]_e$ causes depolarization of the membrane potential by decreasing the driving force for K^+ efflux. (**B**) Statistically significant differences between the steady-state values of the membrane potential (red bars) and the stiffness (gray bars), respectively, before and after increasing the $[K^+]_e$. Cells significantly depolarize and at the same time soften upon increasing extracellular K^+ from 4 to 8 mM.

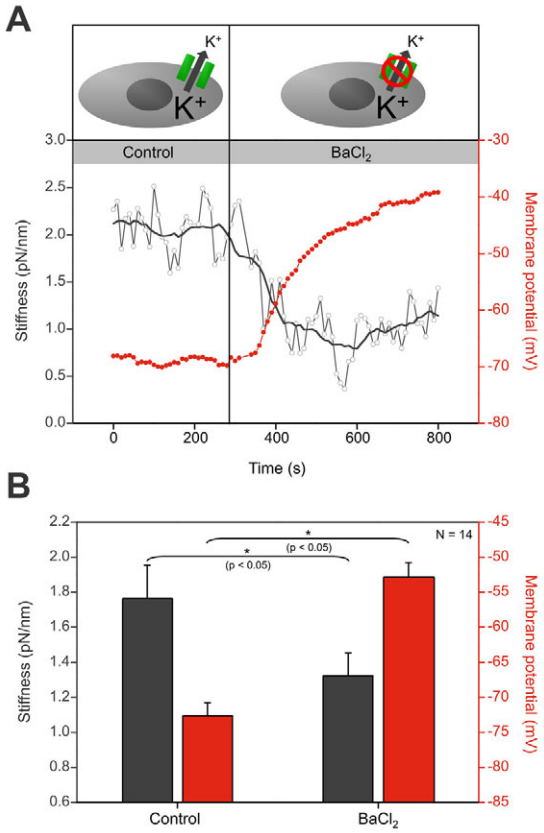

Fig. 2. Effect of K^+ channel blockade by $BaCl_2$ on membrane potential and stiffness. (**A**) Membrane potential (red line) and stiffness (gray line) measurement of a single cell treated with $BaCl_2$. $BaCl_2$-mediated blockade of K^+ channels depolarizes cells by decreasing the permeability of the membrane for K^+. (**B**) Statistically significant differences between the steady-state values of the membrane potential (red bars) and the stiffness (gray bars) before and after application of $BaCl_2$. Cells significantly depolarize and soften upon application of the K^+ channel blocker $BaCl_2$.

accompanying stiffness changes could be reversed upon membrane potential repolarization (data not shown).

Volume changes under low-chloride conditions

It has been previously shown that cell softening can be paralleled by an increase in cell volume (Hillebrand et al., 2007; Hillebrand et al., 2009). Because high $[K^+]_e$, as well as the application of $BaCl_2$ are known to swell endothelial cells (Oberleithner et al., 2009), it was probable that cell softening, caused by either high $[K^+]_e$ or application of $BaCl_2$, was not primarily due to depolarization but due to cell swelling. However, the third depolarizing procedure, namely increasing the outward-directed electrochemical driving force for Cl^-, should not lead to cell swelling but rather to cell shrinkage. In order to test this, we measured endothelial cell height and volume in response to lowering $[Cl^-]_e$ using AFM (Schneider et al., 1997) (Fig. 4). Upon low $[Cl^-]_e$, endothelial cell height decreased from 2.4±0.05 µm to 2.3±0.05 µm after 3 minutes (a change of 5%) and to 2.1±0.05 µm after 9 minutes (a change of 13%). This height decrease nicely mirrored the volume decrease in the cells, namely a decrease in cell volume of 9.2±0.02% after 9 minutes at low $[Cl^-]_e$. Taken together, these results support the idea that cell depolarization rather than swelling is the major determinant for the change in stiffness.

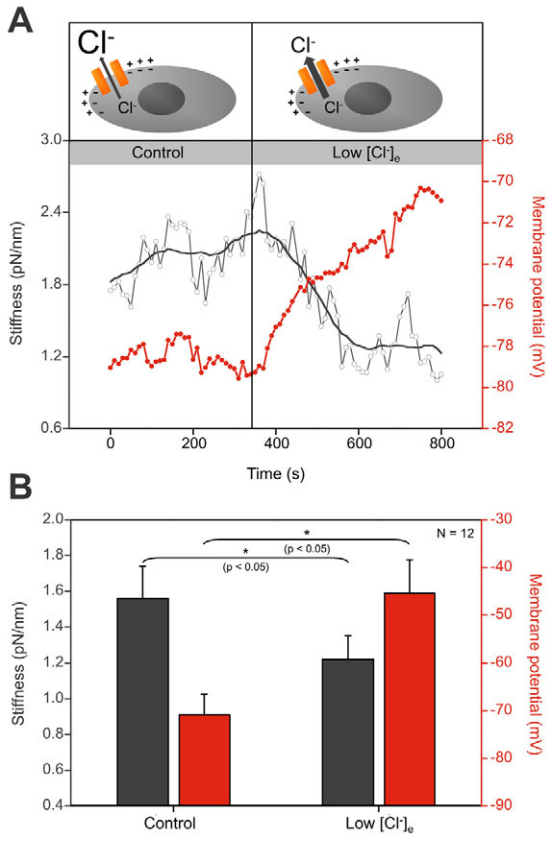

Fig. 3. Effect of low extracellular $[Cl^-]$ on membrane potential and stiffness. (**A**) Tracing of membrane potential (red line) and stiffness changes (gray line) obtained in an individual cell exposed to decreased Cl^- concentrations. Decreasing $[Cl^-]_e$ increases the driving force for Cl^- efflux and thereby depolarizes cells. (**B**) Statistically significant differences between the steady-state values of the membrane potential (red bars) and the stiffness (gray bars) before and after decreasing $[Cl^-]_e$. Lowering $[Cl^-]_e$ significantly depolarizes endothelial cells and again this depolarization is associated with a decrease in cell stiffness.

Effect of cortical actin destabilization on depolarization-induced cell softening

Because it is well known from the literature that cell stiffness is determined in large part by the cortical actin cytoskeleton (Hofmann et al., 1997; Kasas et al., 2005; Oberleithner et al., 2009; Rotsch and Radmacher, 2000; Wakatsuki et al., 2001), it is probable that membrane potential depolarization softens endothelial cells by affecting their actin cortex. In order to test this hypothesis, we depolarized endothelial cells using $BaCl_2$ after disruption of the cortical cytoskeleton by cytochalasin D (Fig. 5). For the experiments, a very low dose of cytochalasin D was used (100 nM) as this concentration was assumed to be low enough to selectively destabilize the submembraneous actin web but not the stress fibers in deeper parts of the cell (Kasas et al., 2005; Oberleithner et al., 2009). In the case that the membrane potential affected cell stiffness through the actin cytoskeleton, cytochalasin D treatment would be expected to abolish the depolarization-induced cell softening. We found that destabilization of cortical actin significantly softens endothelial cells, from 1.7±0.16 pN/nm to 1.0±0.08 pN/nm ($P<0.05$), whereas the membrane potential of the cells remained stable. Importantly, after this cytochalasin-D-mediated cell softening, depolarization of the membrane potential by $BaCl_2$ did not affect cell stiffness (Fig. 5). This finding strongly supports the view that depolarization softens vascular endothelial cells by affecting the cortical actin network.

Discussion

Here, we address the question of whether the electrical plasma membrane potential difference can regulate the mechanical stiffness of vascular endothelial cells. The electrical potential was manipulated in different ways and simultaneously the stiffness of the cells was measured. The electrical potential was modified (i) by changing the electrochemical driving force for K^+ across the plasma membrane, (ii) by blocking membrane K^+ channels by Ba^{2+}, and (iii) by changing the electrochemical driving force for Cl^- across the membrane. K^+ and Cl^- conductances were targeted because it is known that endothelial cells exert both K^+ and Cl^- permeabilities and that these permeabilities are important for setting the endothelial electrical membrane potential (Nilius and Droogmans, 2001). When cells were exposed to high K^+, the membrane potential depolarized. This indicates that the potential difference is governed in part by K^+ channels with Nernst-like behavior and that inward rectifying K^+ channels (K_{ir} channels), which are activated in response to increases in $[K^+]_e$ and thus would have rather hyperpolarized the cells, do not dominate. K_{ir} channels and K^+-induced hyperpolarization have been previously described for endothelial cells (Coldenstanfield et al., 1992; Edwards et al., 1998; Fransen et al., 1995; Jackson, 2005; Nilius and Droogmans, 2001; Vaca et al., 1996; Voets et al., 1996). However, K_{ir} channels obviously exert a minor influence on setting the membrane potential in confluent monolayers. Application of $BaCl_2$ also depolarized the endothelial potential difference, supporting the notion that K^+ channels govern the electrical potential. However, Cl^- conductances seem to play an equally important role for the endothelial membrane potential as a depolarization was also found upon decreasing $[Cl^-]_e$. Simultaneous measurements of the mechanical stiffness then indicated that a decrease of the transmembrane E-field (i.e. a depolarization), independent of the experimental approach (i.e. by changing the electrochemical driving

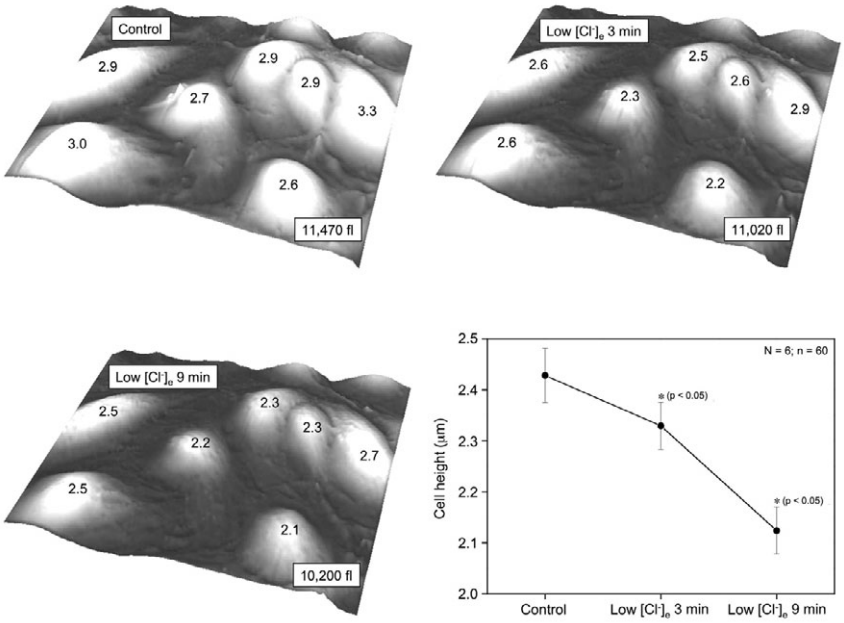

Fig. 4. Volume changes under low Cl^- conditions. AFM height images (100 µm×100 µm) of vascular endothelial cells taken under control conditions and after 3 and 9 minutes under low $[Cl^-]_e$ conditions. Both cell height (given in micrometers on the images and in the graph) and volume [in femtoliters (fl) given at the bottom-right of each image] significantly decrease, indicating shrinkage of endothelial cells upon low $[Cl^-]_e$. Note that the same grayscale code was used in each of the AFM images.

force for K^+, by blocking ion flow through K^+ channels using Ba^{2+} or by altering the driving force for Cl^-) significantly softens endothelial cells. Previously, it has been shown that endothelial cells soften in parallel with an increase in cell volume after application of 17β-estradiol (Hillebrand et al., 2006), the β-adrenoceptor antagonist nebivolol (Hillebrand et al., 2009) or the acute administration of aldosterone (Oberleithner, 2007). On the basis of these experiments it was tempting to speculate that, as a general principle, swollen cells are soft. This view, however, is not supported by the present data because under low Cl^- conditions cells shrink but still soften. Taken together, the high K^+, $BaCl_2$ and low Cl^- experiments therefore indicate that the E-field across the plasma membrane controls cell stiffness.

On the basis of the results described above, the question arises as to how an electrical membrane potential change could influence the mechanical stiffness of a cell. To answer this question, the term mechanical cell stiffness has to be defined in more detail. It is well accepted that the cytoskeleton of the cell, and especially the cortical actin meshwork, plays the predominant role in determining the mechanical strength of a cell. Several studies have shown that promoting depolymerization of filamentous actin (F-actin) by, for example, application of cytochalasins, leads to cell softening (Hofmann et al., 1997; Kasas et al., 2005; Oberleithner et al., 2009; Rotsch and Radmacher, 2000; Wakatsuki et al., 2001). It could, hence, be possible that the membrane potential affects cell stiffness by influencing the polymerization state of cortically located actin filaments; a depolarization would soften the cells by changing the balance between F-actin and G-actin (globular actin) in favor of the latter. This idea is supported by the present results because disruption of the cortical actin meshwork by cytochalasin D abolishes the effect of depolarization on endothelial mechanical stiffness. Likewise, in previous studies it has been shown that K^+ also reduces endothelial cell stiffness by cortical actin depolymerization (Oberleithner et al., 2009).

How in turn could the electrical membrane potential affect the cortical actin cytoskeleton? In many cells, the magnitude of the membrane potential is approx. –70 mV. This does not seem to be

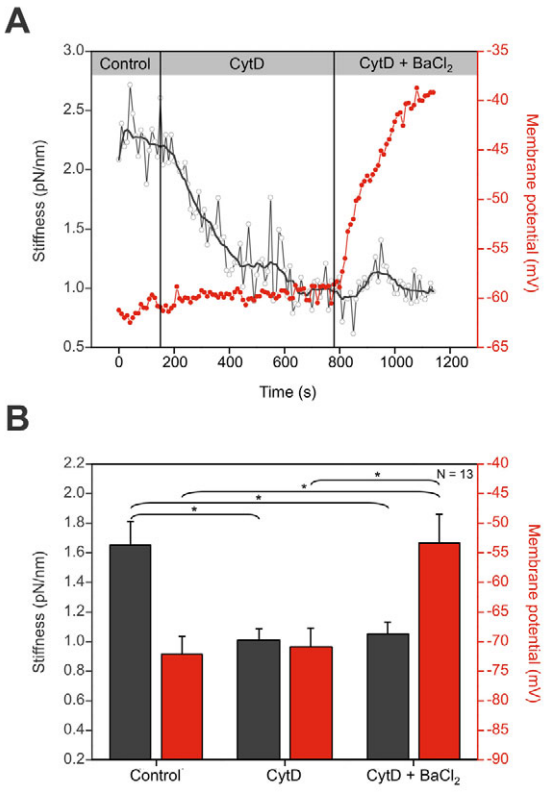

Fig. 5. Effect of cortical actin destabilization on depolarization-induced cell softening. (**A**) Typical measurement of membrane potential (red line) and stiffness (gray line) of a single cell depolarized by $BaCl_2$ after disruption of the cortical actin cytoskeleton by a low dose of cytochalasin D (CytD). (**B**) Statistically significant differences between the steady-state values of the membrane potential (red bars) and the stiffness (gray bars) before and after addition of cytochalasin D and cytochalasin D and $BaCl_2$, respectively. *P<0.05. Cells do not significantly soften upon $BaCl_2$-induced depolarization after cytochalasin D treatment.

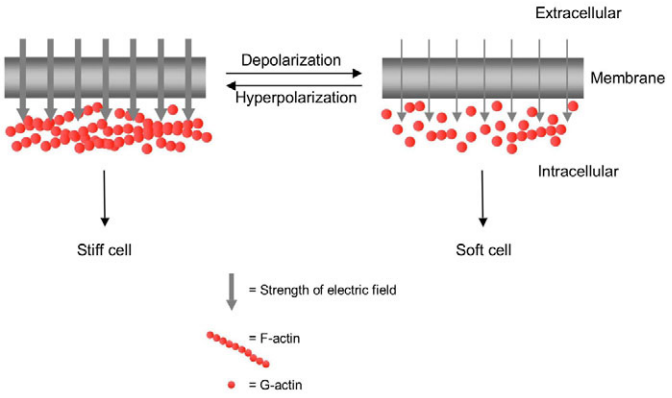

Fig. 6. Model of how a membrane potential change could affect the stiffness of a cell. The stiffness of a cell is determined by the submembraneous actin cytoskeleton. In this model F-actin corresponds to a high stiffness and G-actin to a low stiffness. The membrane potential constitutes a high electrical field at the membrane that can be sensed by the adjacent actin molecules in the cell cortex. A large electrical field, present under hyperpolarized conditions, promotes F-actin formation and thus stiffens cells, whereas depolarization triggers F-actin depolymerization (into G-actin) leading to cell softening.

a high value but, considering the thickness of the membrane (~5 nm), the E-field at the plasma membrane is 0.07 V per 5×10^{-9} m, which corresponds to 14,000,000 volts per meter. It is, hence, probable that such strong E-fields across the plasma membrane can induce changes in cellular processes. However, the question is, whether the E-field at the plasma membrane can be also 'sensed' by molecules outside the membrane (e.g. by actin filaments in the cell cortex). Very few studies have attempted to measure the distance that membrane E-fields can extend into the cell cytosol and this distance is, therefore, largely unknown. However, in a study using 'nanosized voltmeters' inside cells, it has been demonstrated that E-fields arising from membranes can extend out a few micrometers into the cell cytosol (Tyner et al., 2007) and not only ~1–10 nm, as calculated previously (Kamp et al., 1988; Olivotto et al., 1996). Therefore, actin molecules located in the cell cortex could sense changes in the E-field. Changes in the E-field could then affect actin polymerization, as has been proposed previously (Bernstein and Bamburg, 1985; Cantiello et al., 1991; Luther and Peng, 1983; Meggs, 1990); a strong E-field (as is present in case of a hyperpolarized membrane) would be expected to promote actin polymerization, whereas a weakening of the field (as it is the case upon membrane depolarization) would lead to actin depolymerization (Luther and Peng, 1983) (Fig. 6). The latter could explain the softening of the cells observed in this paper. Membrane potential changes could of course also influence actin cytoskeletal dynamics more indirectly by affecting various actin-binding proteins. In this regard, certain intracellular signaling molecules that regulate actin-binding proteins, such as the small GTPase Rho (Waheed et al., 2010), the phosphatidylinositol phosphatase Ci-VSP (Murata and Okamura, 2007) and Ca^{2+} (Nilius and Droogmans, 2001), have already been shown to be influenced by the magnitude of the cell membrane potential.

Depolarization-induced endothelial cell softening, as found in this paper, could play a physiological role in flow-mediated vasodilation, a process in the course of which conduit arteries dilate in response to increased blood flow (Pohl et al., 1986). It is mediated by the endothelium, which, among other paracrines, generates NO (Kelm, 2002). Endothelial cells sense the forces exerted by the blood flow as it activates different plasma membrane ion channels that control the cell membrane potential (Barakat et al., 2006). A typical response of endothelial cells to blood flow is a membrane potential depolarization due to the activation of Cl^--selective ion channels (Barakat et al., 1999; Barakat et al., 2006; Gautam et al., 2006; Qiu et al., 2003). So far, it has not yet been fully clear how this flow-induced depolarization could lead to the upregulation of NO production. In fact, it was thought that a depolarization should decrease NO release as it lowers the driving force for Ca^{2+} influx, which, in turn, should decrease the activity of the Ca^{2+}-dependent endothelial nitric oxide synthase (Cannell and Sage, 1989; Laskey et al., 1990; Lückhoff and Busse, 1990). It has not yet been shown whether flow, as such, changes the submembraneous stiffness of endothelial cells. However, on the basis of the results presented here, it is probable that the depolarization caused by flow softens the endothelial cell cortex and this could account for the increase in NO production.

Materials and Methods

Endothelial cell culture

Bovine aortic endothelial GM 7373 cells (Grinspan et al., 1983) (DSMZ, Braunschweig, Germany) were grown in culture using a procedure similar to that described elsewhere (Oberleithner et al., 2007). Briefly, cells (passage 6 to 10) were cultivated in T_{25} culture flasks using minimal essential medium (MEM) (Invitrogen) with the addition of 1% MEM vitamins, penicillin G (10,000 units per ml), streptomycin (10,000 µg/ml) (Biochrom AG), 1% non-essential amino acids (NEAA) and 20% FBS (fetal bovine serum) (PAA Clone). After reaching confluence, cells were split using trypsin and then cultured at 37°C, under 5% CO_2 on 4-cm glass-bottomed dishes (Willco Wells), in the same culture medium. After 48 hours, confluent cells were used for an experiment.

Solutions and reagents

All drugs and reagents were from Sigma–Aldrich unless otherwise specified. The solutions used were as follows: control solution, HEPES-buffered solution (10 mM HEPES pH 7.4, 140 mM NaCl, 5 mM KCl, 1 mM $MgCl_2$ and 1 mM $CaCl_2$) with respective amounts of solvents; K^+ solutions, HEPES-buffered solution with either 4 or 8 mM KCl (the 4 mM KCl solution was osmotically balanced by addition of mannitol); $BaCl_2$ solution, HEPES-buffered solution with 100 µM $BaCl_2$; low Cl^- solution, HEPES-buffered solution with 140 mM sodium gluconate instead of 140 mM NaCl and supplemented with 4 mM $CaCl_2$; cytochalasin D solution, HEPES-buffered solution with 100 nM cytochalasin D (from a stock solution of 1 mM in 100% ethanol); and calibration solutions, HEPES-buffered solution with either 2, 7.9 or 35 mM NaCl and the respective amounts of *N*-methyl-D-glucamine ($NMDG^+$) (i.e. 138, 132.1 and 105 mM) and 1 µM gramicidin (from a stock solution of 5 mM in 100% ethanol). For membrane potential measurements all solutions were supplied with 1 µM bis-oxonol (from a stock solution of 5 mM in 100% DMSO).

Simultaneous AFM stiffness- and fluorescence-based potential measurements

In order to correlate induced membrane potential changes with the corresponding stiffness changes, we used combined AFM and optical microscopy (Frankel et al., 2006; Haupt et al., 2006; Kellermayer et al., 2006; Liu et al., 2006; Madl et al., 2006; Mathur et al., 2000) and a method that was recently developed in our laboratory and is described in more detail elsewhere (Callies et al., 2009). The stiffness of an individual living cell was assessed using AFM with a 10-µm-diameter spherical tip (Novascan, Ames, IA, USA) as a mechanical nanosensor (Heinz and Hoh, 1999; Kasas and Dietler, 2008) approaching the cell from the top (Fig. 7). The tip then contacts the cantilever and finally indents the cell membrane for a certain distance. Upon indentation, the cantilever (MLCT contact microlever, nominal spring constant of 0.01 N/m; Bruker, Mannheim, Germany), onto which the AFM tip is mounted, bends. This cantilever bending is amplified through a laser beam projected onto the back of the cantilever and the reflected beam is then monitored by a photodiode. Finally, the AFM tip is retracted from the cell again and a new approach–retraction cycle begins so that continuous (every 10 seconds; 0.25 Hz + 6 seconds delay due to retraction) stiffness measurements can be taken. The output of such a stiffness measurement is a force-distance curve, plotting the bending of the cantilever (or the applied force) as a function of the position of the sample (i.e. the piezo) (Fig. 7). From the linear slope of this curve, one can assess whether a cell is rather soft or stiff. For quantification of cell stiffness, the force–distance curve is further transformed into a so-called indentation curve. This is done by subtracting the force–distance curve that had been obtained for the sample from one that had been recorded for a hard surface (e.g. glass) (not shown). The slope of the indentation curve then directly

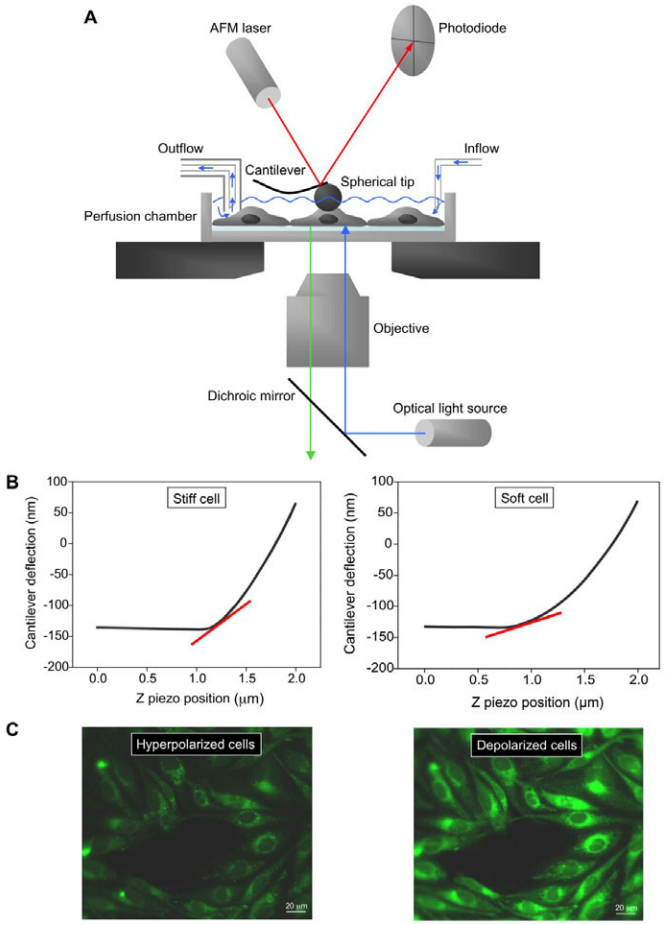

Fig. 7. Combined AFM and fluorescence setup for simultaneous stiffness and membrane potential recordings. (**A**) The spherical AFM tip approaches the cell from the top and continuously generates force–distance curves on the cell. At the same time as stiffness is recorded, the optical microscope collects cellular bis-oxonol fluorescence from the bottom. A perfusion system, designed for the combined AFM and fluorescence setup allows smooth solution changes. (**B**) The cellular stiffness is determined from the slope of a force–distance curve. A steep slope corresponds to a stiff cell and a flat slope to a soft cell. The first detectable linear slope of the curve is depicted in red. This corresponds to the stiffness of the cortical actin cytoskeleton and was used for our analyses. However, other linear slopes can be detected in a force curve. They represent the stiffness of deeper parts of the cell (not used in this study). (**C**) Membrane potential is determined from intracellular bis-oxonol fluorescence intensity. Fluorescence intensity of hyperpolarized cells is low, whereas depolarized cells exhibit high bis-oxonol fluorescence.

reflects the force (in pico- or nano-Newtons), defined as the stiffness, that is required to push the tip into a defined depth of the cell.

At the same time as the stiffness of an individual cell was continuously recorded, the electrical membrane potential of the same cell was assessed using the membrane-potential sensitive fluorescent dye bis-oxonol {bis-(1,3-dibutylbarbituric acid)trimethineoxonol [DiBAC$_4$(3)]}. A light-pulse was applied every 10 seconds through an inverted fluorescence microscope that was integrated into the atomic force microscope (Bioscope Catalyst AFM; Bruker, Mannheim, Germany combined with Leica DMI 6000B; Leica Microsystems, Wetzlar, Germany) (Fig. 7). Bis-oxonol dyes have been extensively used to optically determine the plasma membrane potential of various cell types, including endothelial cells (DallAsta et al., 1997; He and Curry, 1995; Sguilla et al., 2003; Simon et al., 2009). They belong to the slow-response voltage-dependent dyes and distribute between the extracellular space and the cell cytosol in a manner dependent on the magnitude of the electrical plasma membrane potential difference. As bis-oxonol is an anionic (but lipophilic) molecule; more dye enters the cell upon depolarization, where it binds to intracellular components and, hence, cytosolic bis-oxonol fluorescence intensity increases, whereas upon hyperpolarization less dye is located intracellularly and fluorescence intensity is low (Bräuner et al., 1984; Epps et al., 1994) (Fig. 7). Bis-oxonol is considered non-toxic and exhibits large changes in fluorescence intensity in response to potential changes (~1% per mV) (DallAsta et al., 1997). The excitation wavelength for bis-oxonol measurements was 480 nm, whereas fluorescence emission was monitored at 527 nm. The excitation time was 55 mseconds in all experiments and images were collected under 40× magnification. Background values were always subtracted.

In order to quantify the electrical membrane potential after each experiment, cells were subjected to the sodium and potassium ionophore gramicidin and stepwise increases of the extracellular Na^+ concentrations (from 2 to 35 mM) while osmolality was kept constant by addition of respective amounts of the membrane-impermeable cation $NMDG^+$. Assuming that there was no active transport of $NMDG^+$ across the plasma membrane and that gramicidin equally increases the membrane permeability for sodium and potassium, the membrane potentials, corresponding to the respective Na^+ concentrations, were then calculated with the help of the Goldman equation and a calibration curve was generated (not shown).

In order to keep the cells under near-physiological conditions, and for solution changes, the combined AFM:fluorescence setup contained a specially designed perfusion system that did not interfere with the noise-sensitive stiffness measurements (Fig. 7). The bath volume of this perfusion chamber was 2.5 ml and the cells were superfused at a constant rate of 2.5 ml per minute.

AFM volume measurements

The method of imaging the surface of cells with AFM and thereby determining cell height and volume has been previously described in detail (Henderson and Oberleithner, 2000; Oberleithner et al., 2003; Schneider et al., 1997; Schneider et al., 2004). In short, AFM images of living cells in fluid were taken using the Bioscope Catalyst AFM (Bruker, Mannheim, Germany). Cantilevers with colloidal tips (1 µm sphere diameter) and spring constants of ~0.01 pN/nm (MLCT contact microlever, Veeco, Mannheim, Germany; spheres: Novascan, Ames, IA, USA) were used for surface imaging. The rather large spherical tip (in comparison with an AFM tip, which is shaped as a cone) and the low-spring constant of the cantilever assured that the applied indentation force did not compromise the cell height measurements. Surface profiles (128×128 pixels) were obtained with scan sizes of 10,000 m^2 at a scan rate of 3 Hz.

Data collection and statistical analysis

AFM data were collected using the Nanoscope v7.30 software (Bruker, Mannheim, Germany). Stiffness of the cells was calculated with the Protein Unfolding and Nano-Indentation Analysis Software (PUNIAS) (http://site.viola.fr/punias). We analyzed the first part (~100 nm) of the force curve, as this part is known to correspond to the cortical actin cytoskeleton (Kasas et al., 2005; Oberleithner et al., 2009). Individual endothelial cell height (in micrometers) was determined from the plane-fitted (order 1) height images, using the Nanoscope v.7.30 software. Cell volumes were calculated with the help of the Scanning Probe Image Processor (SPIP) software. Bis-oxonol fluorescence intensities were analyzed with Leica LAS AF software 1.7.0 (Leica Microsystems, Wetzlar, Germany). Statistical significant differences were obtained using a paired *t*-test in cases of parametric data and the paired sample Wilcoxon signed rank test in cases where the data were not normally distributed.

This study was supported by grants from the Innovative Medizinische Forschung (OB510901 and SH 510903) and the Deutsche Forschungsgemeinschaft (OB63/17-1 and Kosseleck grant OB 63/18). We thank A. Kolkmann from the mechanics department of the Medical Faculty, University of Münster, for the construction of a perfusion system for the combined AFM and fluorescence setup.

References

Ali, M. H. and Schumacker, P. T. (2002). Endothelial responses to mechanical stress: where is the mechanosensor? *Crit. Care Med.* **30**, 198-206.

Barakat, A. I., Leaver, E. V., Pappone, P. A. and Davies, P. F. (1999). A flow-activated chloride-selective membrane current in vascular endothelial cells. *Circ. Res.* **85**, 820-828.

Barakat, A. I., Lieu, D. K. and Gojova, A. (2006). Secrets of the code: do vascular endothelial cells use ion channels to decipher complex flow signals? *Biomaterials.* **27**, 671-678.

Bernstein, B. W. and Bamburg, J. R. (1985). Reorganization of actin in depolarized synaptosomes. *J. Neurosci.* **5**, 2565-2569.

Bräuner, T., Hülser, D. F. and Strasser, R. J. (1984). Comparative measurements of membrane potentials with microelectrodes and voltage-sensitive dyes. *Biochim. Biophys. Acta* **771**, 208-216.

Califano, J. P. and Reinhart-King, C. A. (2010). Exogenous and endogenous force regulation of endothelial cell behaviour. *J. Biomech.* **43**, 79-86.

Callies, C., Schön, P., Liashkovich, I., Stock, C., Kusche-Vihrog, K., Fels, J., Sträter, A. S. and Oberleithner, H. (2009). Simultaneous mechanical stiffness and electrical potential measurements of living vascular endothelial cells using combined atomic force and epifluorescence microscopy. *Nanotechnology* **20**, 175104.

Cannell, M. B. and Sage, S. O. (1989). Bradykinin-evoked changes in cytosolic calcium and membrane currents in cultured bovine pulmonary artery endothelial cells. *J. Physiol.* **419**, 555-568.

Cantiello, H. F., Patenaude, C. and Zaner, K. (1991). Osmotically induced electrical signals from actin filaments. *Biophys. J.* **59**, 1284-1289.

Chifflet, S., Hernández, J. A., Grasso, S. and Cirillo, A. (2003). Nonspecific depolarization of the membrane potential induces cytoskeletal modifications of bovine corneal endothelial cells in culture. *Exp. Cell Res.* **282**, 1-13.

Coldenstanfield, M., Cramer, E. B. and Gallin, E. K. (1992). Comparison of apical and basal surfaces of confluent endothelial cells: patch-clamp and viral studies. *Am. J. Physiol.* **263**, 573-583.

DallAsta, V., Gatti, R., Orlandini, G., Rossi, P. A., Rotoli, B. M., Sala, R., Bussolati, O. and Gazzola, G. C. (1997). Membrane potential changes visualized in complete growth media through confocal laser scanning microscopy in bis-oxonol-loaded cells. *Exp. Cell Res.* **231**, 260-268.

Edwards, G., Dora, K. A., Gardener, M. J., Garland, C. J. and Weston, A. H. (1998). K^+ is an endothelium-derived hyperpolarizing factor in rat arteries. *Nature* **396**, 269-272.

Epps, D. E., Wolfe, M. L. and Groppi, V. (1994). Characterization of the steady-state and dynamic fluorescence properties of the potential-sensitive dye bis-(1,3-dibutylbarbituric acid)trimethine oxonol ($DiBAC_4(3)$) in model systems and cells. *Chem. Phys. Lipids* **69**, 137-150.

Fels, J., Callies, C., Kusche-Vihrog, K. and Oberleithner, H. (2010). Nitric oxide release follows endothelial nanomechanics and not vice versa. *Pflugers Arch.* **460**, 915-923.

Frankel, D. J., Pfeiffer, J. R., Surviladze, Z., Johnson, A. E., Oliver, J. M., Wilson, B. S. and Burns, A. R. (2006). Revealing the topography of cellular membrane domains by combined atomic force/fluorescence imaging. *Biophys. J.* **90**, 2404-2413.

Fransen, P. F., Demolder, M. J. and Brutsaert, D. L. (1995). Whole-cell membrane currents in cultured pig endocardial endothelial cells. *Am. J. Physiol.* **37**, 2036-2047.

Gautam, M., Shen, Y., Thirkill, T. L., Douglas, G. C. and Barakat, A. I. (2006). Flow-activated chloride channels in vascular endothelium-shear stress sensitivity, desensitization dynamics, and physiological implications. *J. Biol. Chem.* **281**, 36492-36500.

Grinspan, J. B., Müller, S. N. and Levine, E. M. (1983). Bovine endothelial cells transformed in vitro by benzo(A)pyrene. *J. Cell. Physiol.* **114**, 328-338.

Haupt, B. J., Pelling, A. E. and Horton, M. A. (2006). Integrated confocal and scanning probe microscopy for biomedical research. *ScientificWorldJournal*. **6**, 1609-1618.

He, P. and Curry, F. E. (1995). Measurement of membrane potential in endothelial cells in single perfused microvessels. *Microvasc. Res.* **50**, 183-198.

Heinz, W. F. and Hoh, J. H. (1999). Spatially resolved force spectroscopy of biological surfaces using the atomic force microscope. *Trends Biotechnol.* **17**, 143-150.

Henderson, R. M. and Oberleithner, H. (2000). Pushing, dragging, and vibrating renal epithelia by using atomic force microscopy. *Am. J. Physiol. Renal Physiol.* **278**, 689-701.

Hillebrand, U., Hausberg, M., Stock, C., Shahin, V., Nikova, D., Riethmüller, C., Kliche, K., Ludwig, T., Schillers, H., Schneider, S. W. et al. (2006). 17 beta-estradiol increases volume, apical surface and elasticity of human endothelium mediated by Na^+/H^+ exchange. *Cardiovasc. Res.* **69**, 916-924.

Hillebrand, U., Schillers, H., Riethmüller, C., Stock, C., Wilhelmi, M., Oberleithner, H. and Hausberg, M. (2007). Dose-dependent endothelial cell growth and stiffening by aldosterone: endothelial protection by eplerenone *J. Hypertens.* **25**, 639-647.

Hillebrand, U., Lang, D., Telgmann, R. G., Hagedorn, C., Reuter, S., Kliche, K., Stock, C. M., Oberleithner, H., Pavenstadt, H., Bussemaker, E. et al. (2009). Nebivolol decreases endothelial cell stiffness via the estrogen receptor beta: a nano-imaging study. *J. Hypertens.* **27**, 517-526.

Hofmann, U. G., Rotsch, C., Parak, W. J. and Radmacher, M. (1997). Investigating the cytoskeleton of chicken cardiocytes with the atomic force microscope. *J. Struct. Biol.* **119**, 84-91.

Jackson, W. F. (2005). Potassium channels in the peripheral microcirculation. *Microcirculation* **12**, 113-127.

Kamp, F., Chen, Y. D. and Westerhoff, H. V. (1988). Energization induced redistribution of charge carriers near membranes. *Biophys. Chem.* **30**, 113-132.

Kasas, S. and Dietler, G. (2008). Probing nanomechanical properties from biomolecules to living cells. *Pflugers Arch.* **456**, 13-27.

Kasas, S., Wang, X., Hirling, H., Marsault, R., Huni, B., Yersin, A., Regazzi, R., Grenningloh, G., Riederer, B., Forro, L. et al. (2005). Superficial and deep changes of cellular mechanical properties following cytoskeleton disassembly. *Cell Motil. Cytoskeleton* **62**, 124-132.

Kellermayer, M. S., Karsai, A., Kengyel, A., Nagy, A., Bianco, P., Huber, T., Kulcsar, A., Wiedetzky, C., Proksch, P. and Grama, L. (2006). Spatially and temporally synchronized atomic force and total internal reflection fluorescence microscopy for imaging and manipulating cells and biomolecules. *Biophys. J.* **91**, 2665-2677.

Kelm, M. (2002). Flow-mediated dilatation in human circulation: diagnostic and therapeutic aspects. *Am. J. Physiol. Heart Circ. Physiol.* **282**, H1-H5.

Kidoaki, S. and Matsuda, T. (2007). Shape-engineered vascular endothelial cells: nitric oxide production, cell elasticity, and actin cytoskeletal features. *J. Biomed. Mater. Res. A* **81**, 728-735.

Kusche-Vihrog, K., Callies, C., Fels, J. and Oberleithner, H. (2010). The epithelial sodium channel: Mediator of the aldosterone response in the vascular endothelium? *Steroids* **75**, 544-549.

Laskey, R. E., Adams, D. J., Johns, A., Rubanyi, G. M. and Vanbreemen, C. (1990). Membrane potential and Na^+-K^+ pump activity modulate resting and bradykinin-stimulated changes in cytosolic free calcium in cultured endothelial cells from bovine atria. *J. Biol. Chem.* **265**, 2613-2619.

Liu, W., Jawerth, L. M., Sparks, E. A., Falvo, M. R., Hantgan, R. R., Superfine, R., Lord, S. T. and Guthold, M. (2006). Fibrin fibers have extraordinary extensibility and elasticity. *Science* **313**, 634.

Lückhoff, A. and Busse, R. (1990). Calcium influx into endothelial cells and formation of endothelium-derived relaxing factor is controlled by the membrane potential. *Pflugers Arch.* **416**, 305-311.

Luther, P. W. and Peng, H. B. (1983). Changes in cell shape and actin distribution induced by constant electric fields. *Nature* **303**, 61-64.

Madl, J., Rhode, S., Stangl, H., Stockinger, H., Hinterdorfer, P., Schütz, G. J. and Kada, G. (2006). A combined optical and atomic force microscope for live cell investigations. *Ultramicroscopy* **106**, 645-651.

Malek, A. M. and Izumo, S. (1996). Mechanism of endothelial cell shape change and cytoskeletal remodelling in response to fluid shear stress. *J. Cell Sci.* **109**, 713-726.

Mathur, A. B., Truskey, G. A. and Reichert, W. M. (2000). Atomic force and total internal reflection fluorescence microscopy for the study of force transmission in endothelial cells. *Biophys. J.* **78**, 1725-1735.

Meggs, W. J. (1990). Enhanced polymerization of polar macromolecules by an applied electric field with application to mitosis. *J. Theor. Biol.* **145**, 245-255.

Michiels, C. (2003). Endothelial cell functions. *J. Cell. Physiol.* **196**, 430-443.

Murata, Y. and Okamura, Y. (2007). Depolarization activates the phosphoinositide phosphatase Ci-VSP, as detected in *Xenopus* oocytes coexpressing sensors of PIP_2. *J. Physiol.* **583**, 875-889.

Nilius, B. and Droogmans, G. (2001). Ion channels and their functional role in vascular endothelium. *Physiol. Rev.* **81**, 1415-1459.

Oberleithner, H. (2007). Is the vascular endothelium under the control of aldosterone? Facts and hypothesis. *Pflugers Arch.* **454**, 187-193.

Oberleithner, H., Schneider, S. W., Albermann, L., Hillebrand, U., Ludwig, T., Riethmüller, C., Shahin, V., Schafer, C. and Schillers, H. (2003). Endothelial cell swelling by aldosterone. *J. Membr. Biol.* **196**, 163-172.

Oberleithner, H., Riehtmüller, C., Ludwig, T., Shahin, V., Stock, C., Schwab, A., Hausberg, M., Kusche, K. and Schillers, H. (2006). Differential action of steroid hormones on human endothelium. *J. Cell Sci.* **119**, 1926-1932.

Oberleithner, H., Riethmüller, C., Schillers, H., MacGregor, G. A., de Wardener, H. E. and Hausberg, M. (2007). Plasma sodium stiffens vascular endothelium and reduces nitric oxide release. *Proc. Natl. Acad. Sci. USA* **104**, 16281-16286.

Oberleithner, H., Callies, C., Kusche-Vihrog, K., Schillers, H., Shahin, V., Riethmüller, C., MacGregor, G. A. and de Wardener, H. E. (2009). Potassium softens vascular endothelium and increases nitric oxide release. *Proc. Natl. Acad. Sci. USA* **106**, 2829-2834.

Olivotto, M., Arcangeli, A., Carla, M. and Wanke, E. (1996). Electric fields at the plasma membrane level: a neglected element in the mechanisms of cell signalling. *Bioessays* **18**, 495-504.

Pohl, U., Holtz, J., Busse, R. and Bassenge, E. (1986). Crucial role of endothelium in the vasodilator response to increased flow in vivo. *Hypertension* **8**, 37-44.

Qiu, W. P., Hu, Q. H., Paolocci, N., Ziegelstein, R. C. and Kass, D. A. (2003). Differential effects of pulsatile versus steady flow on coronary endothelial membrane potential. *Am. J. Physiol. Heart Circ. Physiol.* **285**, 341-346.

Rotsch, C. and Radmacher, M. (2000). Drug-induced changes of cytoskeletal structure and mechanics in fibroblasts: an atomic force microscopy study. *Biophys. J.* **78**, 520-535.

Schneider, S. W., Yano, Y., Sumpio, B. E., Jena, B. P., Geibel, J. P., Gekle, M. and Oberleithner, H. (1997). Rapid aldosterone-induced cell volume increase of endothelial cells measured by the atomic force microscope. *Cell Biol. Int.* **21**, 759-768.

Schneider, S. W., Matzke, R., Radmacher, M. and Oberleithner, H. (2004). Shape and volume of living aldosterone-sensitive cells imaged with the atomic force microscope. *Methods Mol. Biol.* **242**, 255-279.

Sguilla, F. S., Tedesco, A. C. and Bendhack, L. M. (2003). A membrane potential-sensitive dye for vascular smooth muscle cells assays. *Biochem. Biophys. Res. Commun.* **301**, 113-118.

Simon, A., Harrington, E. O., Liu, G. X., Koren, G. and Choudhary, G. (2009). Mechanism of C-type natriuretic peptide-induced endothelial cell hyperpolarization. *Am. J. Physiol. Lung Cell. Mol. Physiol.* **296**, 248-256.

Tyner, K. M., Kopelman, R. and Philbert, M. A. (2007). "Nanosized voltmeter" enables cellular-wide electric field mapping. *Biophys. J.* **93**, 1163-1174.

Vaca, L., Licea, A. and Possani, L. D. (1996). Modulation of cell membrane potential in cultured vascular endothelium. *Am. J. Physiol.* **39**, 819-824.

Voets, T., Droogmans, G. and Nilius, B. (1996). Membrane currents and the resting membrane potential in cultured bovine pulmonary artery endothelial cells. *J. Physiol.* **497**, 95-107.

Waheed, F., Speight, P., Kawai, G., Dan, Q., Kapus, A. and Száski, K. (2010). Extracellular signal-regulated kinase and GEF-H1 mediate depolarization-induced Rho activation and paracellular permeability increase. *Am. J. Physiol. Cell Physiol.* **298**, 1376-1387.

Wakatsuki, T., Schwab, B., Thompson, N. C. and Elson, E. L. (2001). Effects of cytochalasin D and latrunculin B on mechanical properties of cells. *J. Cell Sci.* **114**, 1025-1036.